crystals

MDPI

Article

Nano Nickel-Zirconia: An Effective Catalyst for the Production of Biodiesel from Waste Cooking Oil

Mohammed Rafi Shaik [1], Mujeeb Khan [1], J. V. Shanmukha Kumar [2], Muhammad Ashraf [3], Majad Khan [3,4], Mufsir Kuniyil [1], Mohamed E. Assal [1], Abdulrahman Al-Warthan [1], Mohammed Rafiq H. Siddiqui [5], Aslam Khan [6], Muhammad Nawaz Tahir [3,4,*] and Syed Farooq Adil [1,*]

1 Department of Chemistry, College of Science, King Saud University, P.O. Box 2455, Riyadh 11451, Saudi Arabia
2 Department of Engineering Chemistry, College of Engineering, Koneru Lakshmaiah Education Foundation, Vaddeswaram, Guntur 522 502, Andhra Pradesh, India
3 Department of Chemistry, King Fahd University of Petroleum and Minerals, P.O. Box 5048, Dhahran 31261, Saudi Arabia
4 Interdisciplinary Research Center for Hydrogen and Energy Storage, King Fahd University of Petroleum and Minerals, Dhahran 31261, Saudi Arabia
5 Department of Chemistry, University of Liverpool, Liverpool L69 7ZD, UK
6 King Abdullah Institute for Nanotechnology, King Saud University, Riyadh 11451, Saudi Arabia
* Correspondence: muhammad.tahir@kfupm.edu.sa (M.N.T.); sfadil@ksu.edu.sa (S.F.A.)

Abstract: The utilization of heterogeneous catalysts during the production of biodiesel potentially minimize the cost of processing due to the exclusion of the separation step. The (X wt%)Ni–ZrO_2 (where X = 10, 25 and 50) catalysts prepared through a hydrothermal process were tested for the production of biodiesel by the transesterification of waste cooking oil (WCO) with methanol. The influences of various reaction parameters were systematically optimized. While the physicochemical characteristics of the as-synthesized catalysts were examined using numerous techniques such as FTIR, XRD, TGA BET, EDX, SEM, and HRTEM. Among all the catalysts, (10 wt%)Ni–ZrO_2 exhibited high surface area when compared to the pristine ZrO_2, (25 wt%)Ni–ZrO_2 and (50 wt%)Ni–ZrO_2 nanocatalysts. It may have influenced the catalytic properties of (10 wt%)Ni–ZrO_2, which exhibited maximum catalytic activity with a biodiesel production yield of 90.5% under optimal conditions. Such as 15:1 methanol to oil molar ratio, 10 wt% catalysts to oil ratio, 8 h reaction time and 180 °C reaction temperature. Furthermore, the recovered catalyst was efficiently reused in several repeated experiments, demonstrating marginal loss in its activity after multiple cycles (five times).

Keywords: transesterification; biodiesel; waste cooking oil; nano-catalysts

check for updates

Citation: Shaik, M.R.; Khan, M.; Kumar, J.V.S.; Ashraf, M.; Khan, M.; Kuniyil, M.; Assal, M.E.; Al-Warthan, A.; Siddiqui, M.R.H.; Khan, A.; et al. Nano Nickel-Zirconia: An Effective Catalyst for the Production of Biodiesel from Waste Cooking Oil. *Crystals* **2023**, *13*, 592. https://doi.org/10.3390/cryst13040592

Academic Editor: Andreas Thissen

Received: 3 March 2023
Revised: 24 March 2023
Accepted: 27 March 2023
Published: 31 March 2023

1. Introduction

Over the last few decades, the consumption of petroleum products has incremented significantly because of excessive industrialization and rapid increase in the world population. As a result, the major portion of the energy used in these processes comes from fossil fuels. However, the petroleum reservoirs are depleting quickly, which could lead to the attrition of many fossil fuel-based stocks [1]. Particularly, the increasing demand for fossil fuels in the transportation sector in recent years has seriously affected the rate of depletion of fossil fuels. Therefore, developing alternative technologies based on renewable resources is inevitable [2]. Recently, many research efforts have been devoted to finding a suitable alternative to fossil fuels. The alternative energy option should be competitive from energy efficiency and cost-effectiveness viewpoints [3]. In this pursuit, biofuels/biodiesels are a promising substitute with high energy efficiency, abundant renewable raw materials, and green environmental impact [4,5].

Biodiesel is derived from triglycerides like plant or animal oils or fats [6]. These constituents are mainly comprised of fatty acid alkyl esters (FAAEs), which are typically

generated by the transesterification of triglycerides of lipids with alcohols (low molecular weight) [7]. Compared to mineral diesel, biodiesel is usually considered a better alternative due to its extraordinary properties, including high renewability, effective biodegradability, environment-friendliness, and excellent lubricity. Besides, biodiesel is portable, non-hazardous, safe to use, readily available and free from aromatics and sulfur contents, significantly increasing its demand in transportation and other relevant sectors [8]. Additionally, biodiesel has a high quality of exhaust gas emission because organic carbon is photosynthetic in origin. It also reduces the percentage of CO_2 emission into the atmosphere and has a negative greenhouse effect [9]. Moreover, due to the close resemblances among the properties of biodiesel and petrodiesel, such as similar energy content, cetane number, viscosity, and phase changes, these two can be easily blended and used as effective alternatives in conventional diesel engines.

For the cost-effective production of biodiesel, various economic and ecological parameters need to be considered. Particularly, the feedstock price has a notable effect on the resulting cost of biodiesel. Thus, local feedstocks are usually considered to reduce the cost of transportation. Biodiesel is primarily produced using various vegetable oils, cooking oils, and animal grease. So far, various vegetable oils (edible or non-edible), such as soybean, rapeseed, cotton, peanut, corn, olive, sesame, and sunflower, have been extensively used as feedstocks for biodiesel production. Apart from this, the synthesis of biodiesels can also be achieved by other non-conventional feedstocks, such as waste cooking oils, microalgae, or animal fats, which have been extensively studied by several investigators. Notably, about 350 types of oil-containing crops are potentially used as precursors to synthesize biodiesel [10]. Among these resources, palm, soybean, rapeseed, moringa, coconut, pongamia, neem, jatropha, sunflower, castor oil, jojoba, cotton, rice bran, and microalgae has received great attention from various researchers globally [11–13]. Since these raw materials are rich in triglyceride contents and mainly consume environmental CO_2 during their growth, this renewable source could help in the remediation of environmental pollution [14]. Due to the increased knowledge and advancements in processing the feedstock, universal biodiesel production is predicted to continue to extend in the upcoming years to a significant amount, i.e., increasing from 29.7×10^6 m^3 in 2014 to 39×10^6 m^3 in 2024 [15].

The formation of biodiesel through the transesterification of oil or fat with alcohol is demonstrated in Scheme 1. This reaction produces fatty acid methyl ester, while the ref. [16] glycerol is formed as a byproduct. Mechanistically, transesterification is a reversible process. Therefore, it requires an excess of alcohol which facilitates the shifting of the equilibrium reaction towards the product side. At the same time, chemical catalysts are applied to enhance the reaction kinetics and product yield. During the transesterification reactions, the types and contents of alcohol play a major role. Short-chain alcohols like ethanol, methanol, butanol, and propanol are mostly preferred for this process. Among these alcohols, methanol is the maximum selected alcohol due to its less expensive and physicochemical (polar, short carbon chain) properties [17]. The transesterification reaction could be catalyzed using an alkaline or acidic medium. The alkaline medium with better kinetic is mostly utilized on a commercial scale, even under low amounts of fatty acid [18].

The commercialization of biodiesel is predominantly inhibited by the price of production. So far, biodiesel is still costly when compared to conventional fossil fuels. The cost of raw feedstock oils and the synthesis of catalysts are still considered the main cost of biodiesel production (60–80%) [19]. The former problem could be solved by choosing less expensive and locally available feedstock which are low costs like, waste cooking oil (WCO), animal fats [20], palm fatty acid distillate (PFAD) [21], Jatropha curcas oil [22] and grease etc. [23,24]. Whereas extensive scrutiny is still needed to minimize the cost of catalyst production. In this regard, WCO is a suitable feedstock which is abundantly available and largely considered an environmental pollutant and harmful to health. WCO is a growing menace to the environment and thus needs to be disposed of safely, but it often requires a large amount of management resources for safe disposal. The leftover

WCO usually becomes part of sewerage leaching and significantly contaminates the water resources, affecting human health, animals, plants and most aquatic life [25].

Conventionally, biodiesel production is achieved by employing base catalysts such as sodium hydroxide or potassium hydroxide under homogeneous catalytic conditions. However, this method suffers from various limitations, such as separation, recycling, and regeneration of the catalyst. Moreover, the product should be neutralized with strong acids like hydrochloric acid, phosphoric acid, or sulfuric acid, followed by washing of product with plenty of water. Altogether, the process becomes cost-intensive and environmentally hazardous due to the applications of many inorganic acids and water for post-reaction work-up [26]. Therefore, heterogeneous catalysis qualifies better to solve these problems [27]. The heterogeneous catalysts operate under benign conditions that help in the catalyst's easy separation, recycling, and regeneration.

Moreover, it doesn't require washing and neutralization of reaction contents [28]. Therefore, the process could be scaled-up to meet the market demands. Accordingly, heterogeneous catalysts have become popular for producing biodiesel via transesterification reactions.

Typically, biodiesel production through transesterification of WCO has been reported to be performed by using diversification of heterogeneous catalysts, including mixed metal oxides. For instance, Mohadesi et al. [29] have generated biodiesel in the existence of catalyst (KOH) and small-chain alcohol (methanol). Detailed analysis of the reaction has been performed by varying parameters, including alcohol-to-oil ratio, catalyst contents, reaction duration and temperature. The results have revealed that a methanol to oil ratio of 9.4:1, 1.16 wt% of catalyst, duration of 120 s, and a temperature of 62.4 °C have resulted in the formation of high yield of transesterification product (methyl ester, 98.2%). In another study, Mansir et al. [16] utilized WCO to produce biodiesel in high yield (92.1%) under optimized reaction conditions. They have used ~3 wt% of Mn-Zr (2:3)/CaO as a catalyst, a CH_3OH to oil ratio of 15:1, a temperature of 80 °C and a time of ~3 h. Similarly, Putra and co-workers [30] have reported the preparation of CaO/SiO_2 catalyst using cost-effective raw materials obtained from waste eggshells. When the catalyst was applied for biodiesel production using WCO under appropriate conditions (1 h and 60 °C), a high yield of transesterification product was obtained (~91%). While in another study, Sadaf et al. [31] successfully transformed WCO to biodiesel in high yield (~94%) using KOH (1 wt%), CH_3OH to oil molar ratio of 1:3 at 60 °C. Furthermore, $CaO/KI/\gamma\text{-}Al_2O_3$ catalyst prepared by Asri et al. has demonstrated efficient catalytic activity during the WCO transesterification by facilitating the formation of a high yield of product (83.08%) under optimized conditions, such as ref. [32] 6% of catalyst, 1:15 WCO to CH_3OH ratio, a temperature of 65 °C and a 5 h reaction time.

Apart from these, other commonly applied heterogeneous catalysts are metal oxides [33], zeolites [34] and hydrotalcites etc. [35]. This report presents the synthesis of nickel-zirconium mixed metal oxides (X%)Ni–ZrO_2 with different ratios of Ni(X = 10, 25 and 50 wt%) and its application in the transesterification of WCO as a heterogeneous catalyst. Furthermore, nickel-zirconium-based catalysts have also been used as heterogeneous catalysts in many other organic transformations, such as the hydrogenation of acetonitrile [36], hydrogenation of carbon oxides [37], hydrogenation of tetralin [38], hydrogen production [39] and oxidation of alcohols [40].

The process of transesterification of WCO to biodiesel using nickel-zirconium-based mixed metal oxide catalysts is depicted in Scheme 1. The as-prepared catalyst was identified by using a variety of techniques, including Fourier transform infrared spectra (FT-IR), transmission electron microscopy (TEM), energy dispersive X-ray (EDX), X-ray diffraction (XRD), thermal gravimetric analysis (TGA) and Brunauer Emmett Teller (BET) surface area analysis. Detailed analysis of the catalytic transesterification of WCO was performed to optimize the reaction conditions to obtain the maximum yield of the product. Furthermore, several experiments were performed under similar conditions to test the reusability of the catalysts for the same reaction.

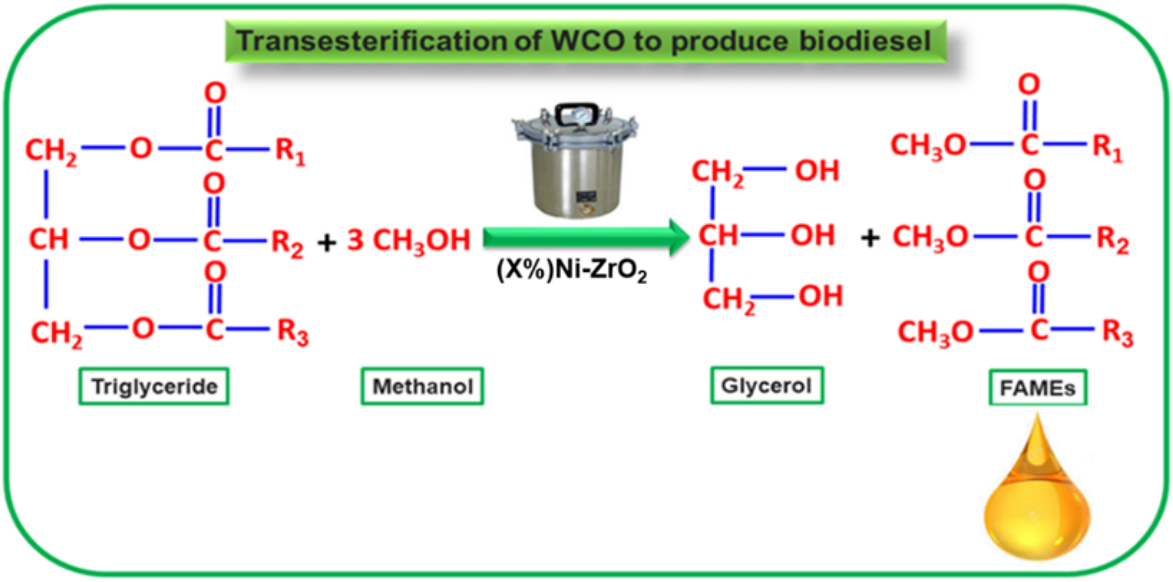

Scheme 1. Schematic diagram of transesterification of WCO to biodiesel using the developed catalyst.

2. Experimental Section

2.1. Catalyst Preparation

Ni–ZrO_2 with different % ratio of Ni was synthesized using the solvothermal method. For example, to synthesize Ni (10 wt%)–ZrO_2, a clear solution of nickel acetylacetonate (0.166 g) in tert. butanol (10 mL) and oleylamine (2 mL) were made in a conical flask by heating at 80 °C. In another flask, a clear solution of zirconium isopropoixde (1.66 g) in benzyl alcohol (15 mL) was taken. Both solutions were mixed and sealed in a Teflon-lined autoclave at 200 °C for 48 h. After the required time, the reaction vessel was brought down to room temperature, and ethanol (50 mL) was added to precipitate the product, which was separated using centrifugation and washed three times by dissolving the precipitates in dichloromethane (10 mL) and precipitating using ethanol (50 mL).

2.2. Transesterification Experiment

To test the catalytic activity of the as-prepared catalyst, WCO (3 g), methanol (15 times molar; molecular weight of oil was considered as 890) and catalyst (10 wt% of oil) were taken into a 100 mL Teflon cup, which was later placed in a stainless-steel autoclave. To complete the reaction, the autoclave was kept in a muffle furnace at a high temperature (180 °C) for 8 h. After this, the autoclave was taken out and allowed to cool down to room temperature. The catalyst was isolated from the reaction mixture using centrifugation (4000 rpm), while the unreacted alcohol was isolated on a rotary evaporator. Subsequently, the reaction mixture only contained trans-esterified products (fatty acid alkyl esters), unreacted oil, and glycerol as a side product. This reaction mixture added 5 mL of hexane to separate the glycerol, which ultimately precipitated out at the bottom of the vessel. The oil and the transesterified product readily went into the organic layer, and glycerol persisted as a discrete layer. The organic layer was separated using a separating funnel, and hexane was distilled using a rotary evaporator. The conversion of the products (fatty acid alkyl esters) was analyzed by ^{1}H NMR spectroscopy.

3. Results and Discussion

X-ray diffraction was used to confirm the catalyst's crystal structure and phase purity. Figure 1 displays the XRD patterns of the synthesized (10 wt%)Ni–ZrO_2, (25 wt%)Ni–ZrO_2 and (50 wt%)Ni–ZrO_2 catalysts. The characteristic reflections observed in the X-ray diffractograms of the samples with different compositions of Ni were situated at 2θ = 44.44°, 51.71° and 76.41° belonged to planes (111), (200) and (220), respectively. This indicates

that the prepared samples contain nickel in a face-centred cubic (*fcc*) form (JCPDS file no. 04-0850). [41] Whereas the reflections at 2θ = 40.00° and 46.58° could appear due to the mixed hexagonal phase of metallic Ni [42]. Besides, the prepared materials exhibited a series of reflections at 2θ = 30.32°, 50.49° and 60.23°, corresponding to (111), (220) and (311) planes for the cubic ZrO_2 structure, which is in high accordance with (JCPDS file no. 27-0997) [43].

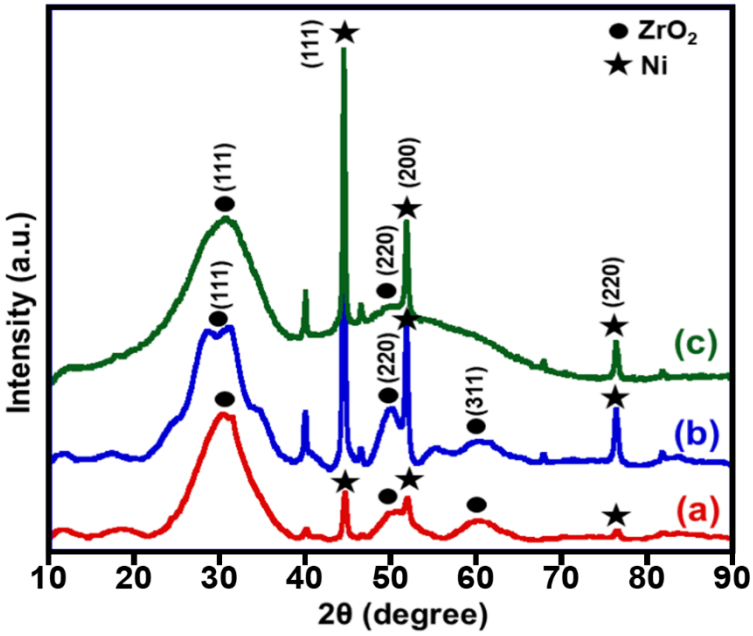

Figure 1. XRD analyses of the (**a**) (10%)Ni–ZrO_2, (**b**) (25%)Ni–ZrO_2 and (**c**) (50%)Ni–ZrO_2 catalysts.

To recognize the functional groups existing on the surface of synthesized nano-catalysts, we characterized the catalysts using FT-IR. FTIR spectra of (10 wt%)Ni–ZrO_2, (25 wt%)Ni–ZrO_2 and (50 wt%)Ni–ZrO_2 are presented in Figure 2. All three samples with different amounts of Ni showed very similar surface functional groups. The major peaks appeared at 3450, 1632, 1560 and 1440 cm^{-1}. These could be assigned to the stretching υ(–OH) and bending δ(–OH) vibration modes of the OH group due to the occurrence of benzyl alcohol which acts as both solvent and surface stabilizing ligand [44]. Meantime, the CH_2 stretching vibration illustrates the sharp absorption bands of nearly 2940 cm^{-1} [45]. The absorption peak situated at 1040 cm^{-1} demonstrates the existence of the stretching vibrations of υ(C−O) [46]. These absorption bands suggest the presence of benzyl alcohol on the surface as stabilizing ligands. The stretching vibration band υ(Zr–O) of zirconia displays the peaks centered approximately at 630 and 740 cm^{-1} [47]. Besides, the FT-IR peaks in the 460–600 cm^{-1} could be due to the stretching vibration modes of υ(Ni–O) [48].

To determine the catalysts' thermal stability, the samples were subjected to Thermal gravimetric analysis at various temperatures. The thermal behavior of the as-synthesized catalyst with compositions (10 wt%)Ni–ZrO_2, (25 wt%)Ni–ZrO_2 and (50 wt%)Ni–ZrO_2 catalysts were studied up to 800 °C with a heating rate of 10 °C min^{-1} under N_2 gas flow, and the results are shown in Figure 3. The TGA thermogram of (50 wt%)Ni–ZrO_2 catalyst was stable up to 340 °C with a slight mass loss of <3%, which can be attributed to the evolution of adsorbed moisture and surface stabilizing ligand on the as-prepared catalyst [47]. After this, a gradual weight loss of ~9% was observed in the temperature range of 400–600 °C. Upon further increasing the temperature to 800 °C, an overall weight loss of ~18% was observed. These analyses have revealed that, upon decreasing the weight percentage of Ni in the composition of the catalyst, i.e., (10 wt%)Ni–ZrO_2 and (25 wt%)Ni–ZrO_2, the thermal stability was considerably decreased. The total weight loss for (10 wt%)Ni–ZrO_2 and (25 wt%)Ni–ZrO_2 was approximately 28% and 40%, respectively.

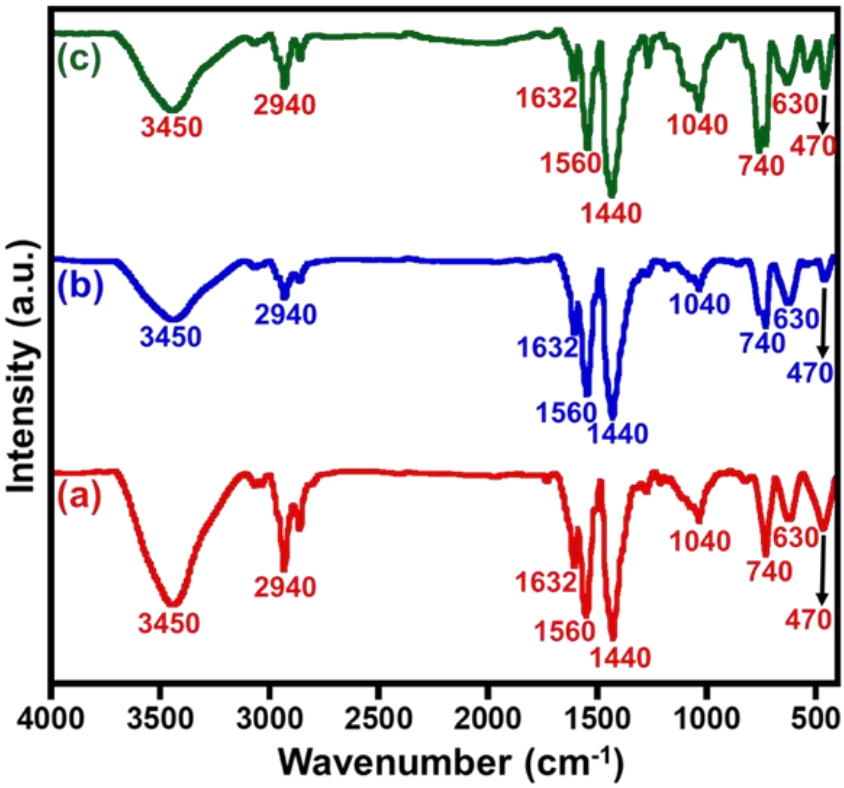

Figure 2. FTIR spectra of the (**a**) (10%)Ni–ZrO_2, (**b**) (25%)Ni–ZrO_2 and (**c**) (50%)Ni–ZrO_2 catalysts.

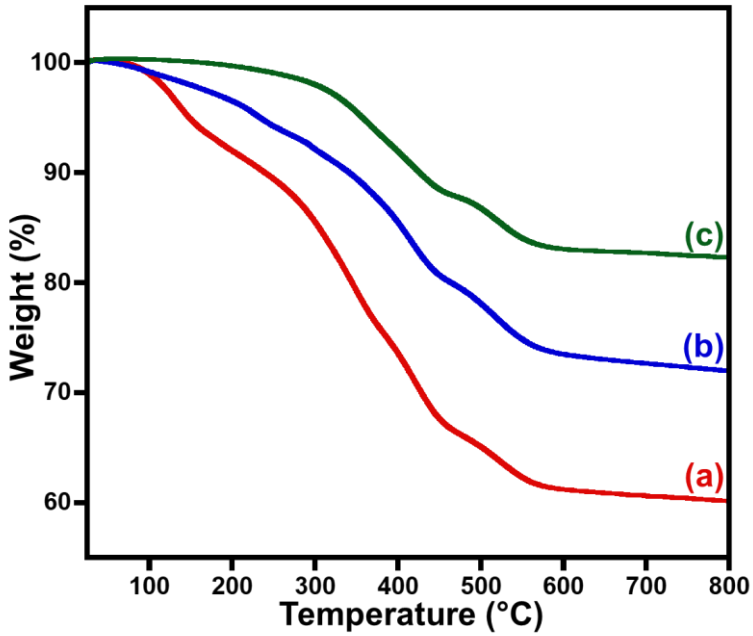

Figure 3. TGA thermograms of the (**a**) (10 wt%)Ni–ZrO_2, (**b**) (25 wt%)Ni–ZrO_2 and (**c**) (50 wt%)Ni–ZrO_2 catalysts.

The synthesized samples' morphology was studied using scanning electron microscopy and transmission electron microscopy. Figure 4 shows the representative SEM images of the (10 wt%)Ni–ZrO_2 (Figure 4a), (25 wt%)Ni–ZrO_2 (Figure 4b), (50 wt%)Ni–ZrO_2 (Figure 4c) and transmission electron microscopy image of (10 wt%)Ni–ZrO_2 (Figure 4d). Although the SEM images show some spherical shape nanoparticles, overall, these particles are beyond the resolution limits of SEM. However, TEM shows small spherical

nanoparticles with very well crystalline domains. Additionally, the elemental mapping of (10 wt%)Ni–ZrO_2 catalyst was confirmed using SEM at the rectangular area in Figure 5. The data disclosed the presence of homogeneously distributed O (turquoise), Ni (yellow) and Zr (red) atoms over the 20 µm sized cross-section area of the image. Moreover, the elemental composition analysis of the as-prepared (10 wt%)Ni–ZrO_2 catalyst is also studied using the EDX technique, as viewed in Figure 5. The existence of zirconium, nickel and oxygen has been indicated in the EDX spectrum.

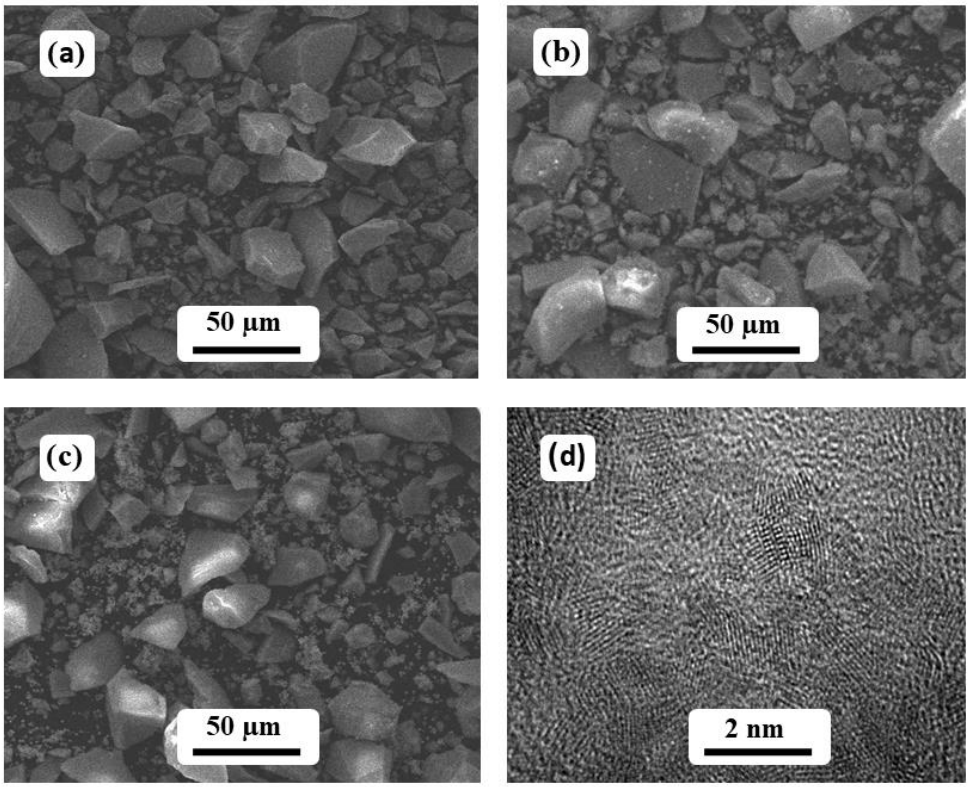

Figure 4. FESEM micrographs of (**a**) (10 wt%)Ni–ZrO_2, (**b**) (25 wt%)Ni–ZrO_2, (**c**) (50 wt%)Ni–ZrO_2 and (**d**) TEM image of (10 wt%)Ni–ZrO_2 catalyst.

The catalysts' surface area was analyzed by BET by taking the surface areas of the pure ZrO_2 as a reference. The BET of (10 wt%)Ni–ZrO_2, (25 wt%)Ni–ZrO_2 and (50 wt%)Ni–ZrO_2 catalysts measured with N_2 adsorption are presented in Figure 6. The transesterification process is highly dependent on the surface area of the heterogeneous catalysts [49,50]. The surface area of pristine ZrO_2 was about 59.72 m^2 g^{-1}, whereas the surface areas of the catalysts, i.e., (10 wt%)Ni–ZrO_2, (25 wt%)Ni–ZrO_2 and (50 wt%)Ni–ZrO_2 catalysts were 117.83, 96.46, and 85.07 m^2 g^{-1}, respectively. The catalytic activity of the catalysts with Ni NPs exhibited higher catalytic efficiency than pure ZrO_2 NPs-based catalysts. The surface area of all the studied catalysts was reduced upon increasing the weight percentage of Ni NPs. The trend of the surface area reduction upon increasing the Ni content can be attributed to the limited obstruction of the catalytically active catalyst sites by the Ni NPs. This, in turn, affects the activity of the prepared catalysts. Interestingly, among various catalysts, the catalyst with the highest surface area, i.e., (10 wt%)Ni–ZrO_2, has exhibited the superior conversion of WCO to biodiesel. Therefore, it can be concluded that the catalytic behavior of the fabricated catalysts is powerfully affected by the specific surface area of the material.

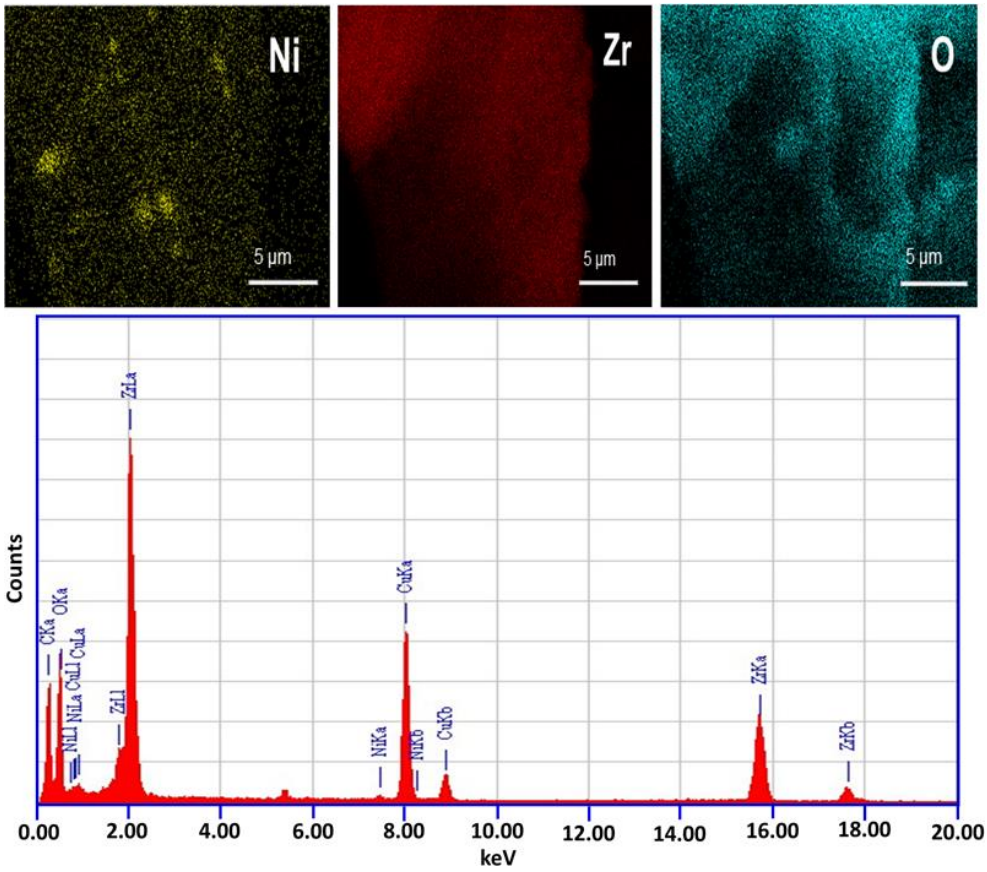

Figure 5. FESEM elemental mapping and elemental analysis (EDX) spectrum of a catalyst (10 wt%) Ni–ZrO_2.

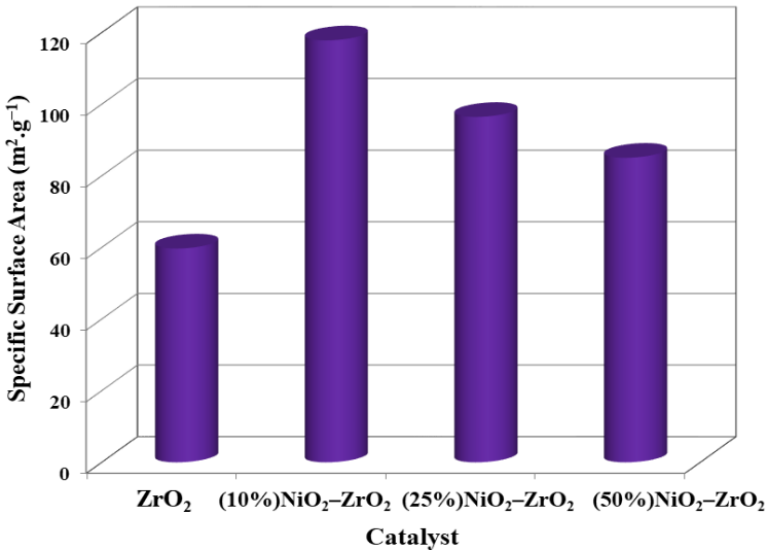

Figure 6. BET surface area results of pure ZrO_2, (10 wt%)Ni–ZrO_2, (25 wt%)Ni–ZrO_2 and (50 wt%)Ni–ZrO_2 catalysts.

3.1. Catalytic Investigation

(10 wt%)Ni–ZrO_2 catalyst was investigated for transesterification using WCO as a feedstock. The product formed during this transesterification reaction was analyzed by using ^{1}H-NMR spectroscopy. A schematic illustration of the process is described in Scheme 2. The NMR spectrum displays two proton peaks at δ = 4.10–4.30 and 5.10 ppm,

which can ascribe to the –CH_2– and –CH– of the glycerol moiety in triglyceride, respectively. In this case, the mono and the -di glycerides of the glyceride moieties were not considered, as these compounds are soluble in MeOH and might have segregated during the separation process. Notably, triglyceride exhibits various chemical shifts due to the effect of couplings from –CH_2– constituents under different chemical environments (δ = 1.30, 1.60, 1.95, 2.30 and 2.63 ppm). These types of all coupling peaks are commonly found in fatty acid methyl ester (FAME) and triglycerides, in addition to the existence of other couplings which occurred due to the non-conjugated and conjugated proton resonances (δ = 5.30, 5.35 and 6.03 ppm). The ^{1}H-NMR spectrum of FAME exhibited a prominent peak at δ 3.65 ppm due to the presence of the methoxy group. This peak was utilized to assess the conversion percentage of biodiesel during the reaction using the equation below [51,52].

$$\text{Conversion}(\%) = 100 \times 2 \times {}^{A_{CH_3}}\!\big/ 3 \times A_{\alpha-CH_2} \quad (1)$$

where A_{CH_3}—area of methoxy protons in the methyl esters, $A_{\alpha-CH_2}$— area of the CH_2 protons adjacent to the carbonyl group.

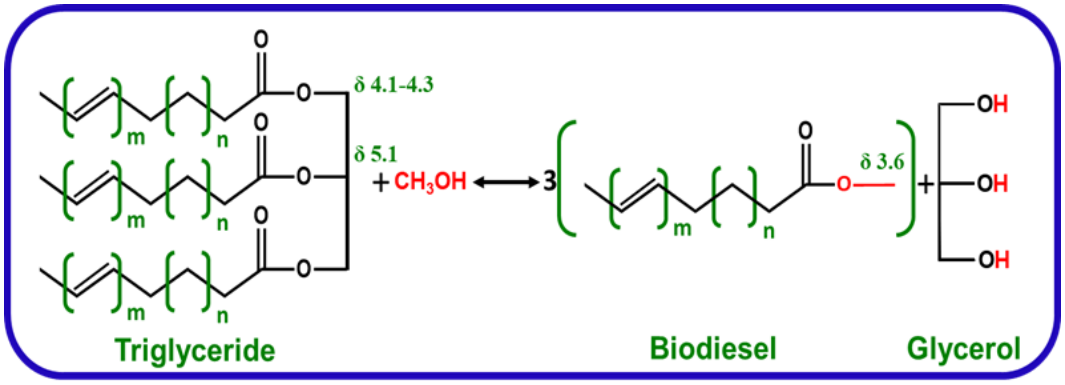

Scheme 2. Schematic diagram of transesterification of a triglyceride with MeOH.

Several experiments were performed to examine the influence of different reaction parameters on the transformation of WCO to biodiesel, such as catalyst loading, molar ratio of MeOH to WCO, duration of the reaction, and temperature of the reaction. These parameters were systematically varied to find the optimum reaction conditions for the production of biodiesel in high yield. The products produced from the transesterification process were analyzed using ^{1}H-NMR spectra by calculating the WCO conversion to biodiesel, which was performed per the outcomes computed from glycerol attained. The conversion obtained from glycerol quantity will be lesser, by 1–5 mol% compared with the NMR results, since the higher glycerol viscosity prohibits the 100% regaining of it from the reaction mixture [53].

3.2. Impact of Catalyst Loading

The catalytic activity of the (X wt%)Ni–ZrO_2 catalysts (where X = 0, 10, 25 and 50) was studied while other catalytic parameters were kept unchanged, i.e., the temperature at 180 °C, MeOH-to-oil ratio15:1, 10 wt% catalysts and reaction temperature of 8 h. The conversion of transesterification of WCO by MeOH was monitored using ^{1}H-NMR spectroscopy. Pure ZrO_2 was also used in the conversion of WCO with MeOH to produce biodiesel; the biodiesel yield was approximately 7.43% under the above-mentioned conditions. However, the presence of 10 wt% of Ni–ZrO_2 catalyst could improve the conversion of WCO up to 90.5%. The enhanced biodiesel yield can be ascribed to the significant improvement in the specific surface area of the catalyst, as illustrated in the BET data [54]. The high surface area of the catalyst allowed better adsorption of the reactants on its surface, which ultimately enhanced the efficiency of the reaction [55]. As shown in Figure 7a, the (10 wt%)Ni–ZrO_2

catalyst exhibits the highest conversion among all three catalysts. The conversion of WCO was gradually decreased by loading more weight percentages of Ni on the ZrO_2 catalyst. The catalysts (25 wt%)Ni–ZrO_2 and (50 wt%)Ni–ZrO_2 yielded 79.2% and 75.0% conversion, respectively. This could be due to the decline in the surface area or blocked active sites upon the addition of Ni, as mentioned earlier. However, the surface area of the synthesized catalyst plays a pivotal role in the catalytic efficiency towards biodiesel production. Therefore, the (10 wt%)Ni–ZrO_2 catalyst was found to be the optimum catalyst, and hence it is employed in future investigations to enhance other catalytic variables.

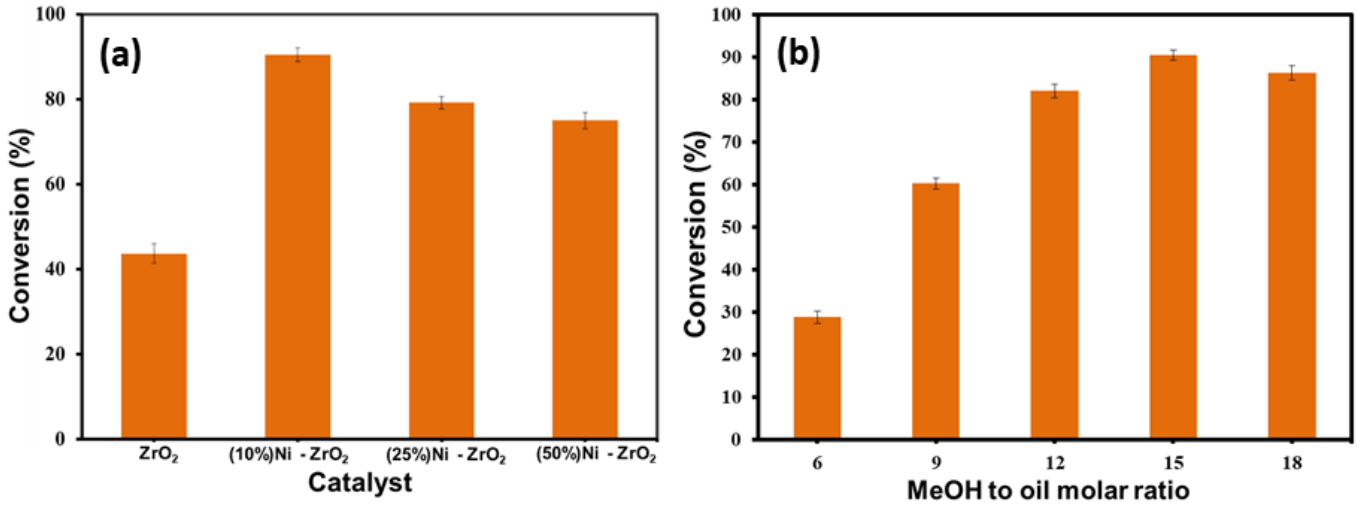

Figure 7. (**a**) Catalytic activities of (X%)Ni–ZrO_2 catalysts for the production of biodiesel from WCO and (**b**) Conversion of WCO at different molar ratios (6:1–18:1), 10 wt% loaded catalyst concentration, 8 h reaction time and 180 °C temperature.

3.3. Impact of Molar Ratio

Among various parameters the methanol amount concerning the oil. i.e., the molar ratio of MeOH to oil is regarded as one of the most crucial factors in the transesterification process, which can potentially inhibit the formation of biodiesel. The common stoichiometric ratio of the transesterification process requires 3 moles of MeOH to generate 3 moles of methyl ester and 1 mole of glycerol. However, as the transesterification process of triglyceride is reversible, an excess volume of MeOH can potentially drive the equilibrium towards the right. Therefore, in these reactions, the methanol to oil molar ratio is higher than that of the stoichiometric ratio of 3:1is maintained. The process was performed by changing methanol to oil molar ratios from 6:1 to 18:1 under unchanged operational conditions (180 °C, 8 h and 10 wt% catalysts to oil ratio), as displayed in Figure 7b. Upon raising the MeOH to oil molar ratio from 6:1 to 15:1, the biodiesel yield was enhanced considerably from 28.8% to 90.5%.

Nevertheless, a further increase in alcohol to oil molar ratio from 15:1 to 18:1 decreased the biodiesel formation. This is probably attributed to the dilution catalyst effect, which led to the insolubility of the MeOH [56]. Therefore, in this study, the prime molar ratio of methanol to WCO was established to be 15:1.

3.4. Impact of Reaction Time

Figure 8 a represents the conversion of WCO at 180 °C for numerous reaction times. Reaction time plays a fundamental role in biodiesel yield, especially for the catalytic transesterification processes. Typically, the rate of reaction is highly dependent on the existence of the catalyst; furthermore, the participation of the mass transfer rate happened during the reaction utilizing a heterogeneous catalyst [57]. As the reaction duration increases, the biodiesel yield increases significantly. A lower WCO conversion of 13.5% was obtained after 2 h. The optimal WCO conversion of 90.5% was achieved when the reaction time

was increased to 8 h. Upon further prolonging the reaction period to 10 h, there was an insignificant decline in the yield of biodiesel. This is typically feasible when the equilibrium is obtained at the optimal biodiesel yield, and the reverse reaction considerably occurs. Besides, some side reactions occur after the optimal reaction time [58,59]. Based on this data, the ideal reaction time for the transesterification procedure in the present study is 8 h.

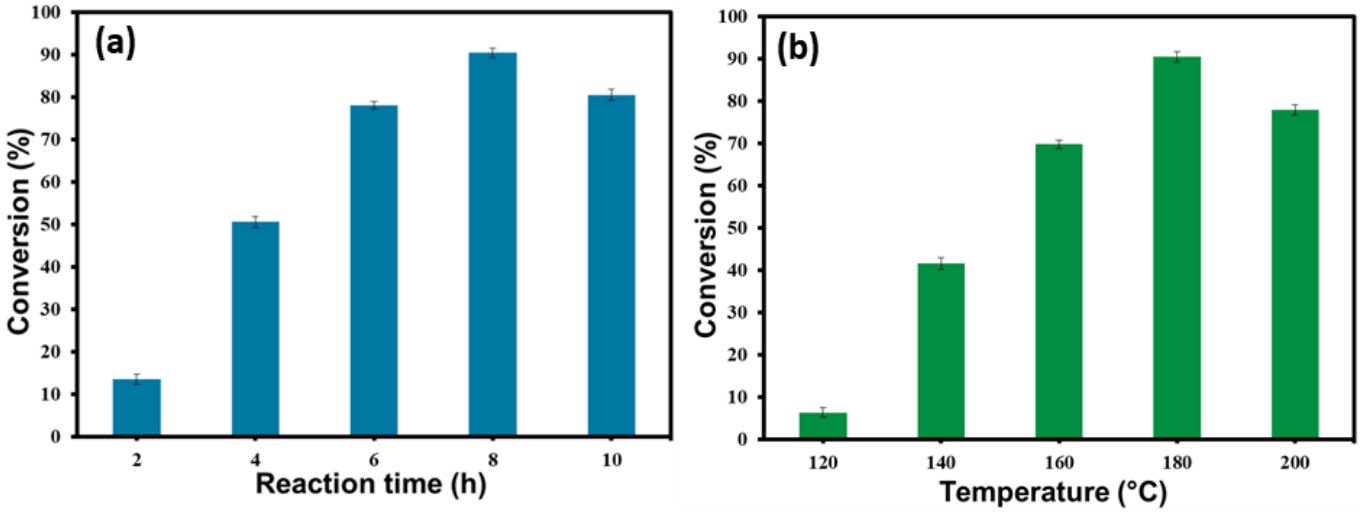

Figure 8. (**a**) Conversion of WCO at different reaction times (2–10 h), 15:1 methanol/oil molar ratio, 10 wt% catalyst concentration and 180 °C temperature and (**b**) Conversion of WCO at different temperatures (120–180 °C), 15:1 molar ratio of methanol:oil, 8 h of reaction time and 10 wt% catalyst concentration.

3.5. Impact of Reaction Temperature

Apart from this, the temperature of the reaction is also a significant factor which can influence the transesterification reaction. Therefore, evaluation of the catalytic performance at different temperatures was carried out under optimized conditions, such as a reaction time of 8 h, 15:1 as MeOH-to-oil ratio and the number of catalysts as 10 wt% of WCO. The increment in the reaction temperature favored the formation of methyl ester, as displayed in Figure 8b. The influence of temperature was also examined on the esterification reaction by varying the temperature from 120 °C to 200 °C. The plotted results showed that the conversion of WCO to methyl ester increased from 6.3% to 90.5% when the upsurge reaction temperature increased from 120 to 180 °C, respectively.

Further reaction temperature upsurge from 180 to 200 °C led to a slight decrease in methyl ester yield. This behavior is per several other published studies which proposed that the saponification process of triglyceride may take place at high temperatures, which subsequently form an enormous number of bubbles that inhibit the reaction on the three phases (alcohol/oil/catalyst) interphase; therefore, decreased the biodiesel yield [60]. Thus, the optimal biodiesel yield can be attained at a temperature of the reaction 180 °C.

3.6. Impact of Catalyst to Oil Ratio

Usually, catalyst concentration remarkably affects the transformation of WCO to biodiesel. An insufficient quantity of the catalyst led to an incomplete transesterification reaction [61]. To assess the influence of catalyst dosage, the quantity of the catalyst was varied from 6 to 14 wt% while keeping the other operational conditions persistent. Upon increasing the catalyst amount, the yield of the biodiesel also upsurges. Since with increasing the quantity of the catalyst, the amount of O^{2-} anion sites also increases, which facilitates the adsorption of more hydrogen ions (H^+) from CH_3OH, leading to the formation of a higher number of active sites [62]. This will ultimately lead to an increased number of contacts between the reactants and the active sites, enhancing the resulting yield of biodiesel. Overall, the increase in catalyst percentage from 6 to 10 wt% resulted in the

conversion from 44.6% to 90.5% (Figure 9a). The results in Figure 9a demonstrate that the conversion of WCO to biodiesel is negatively impacted upon further increasing the amount of catalysts to more than 10%.

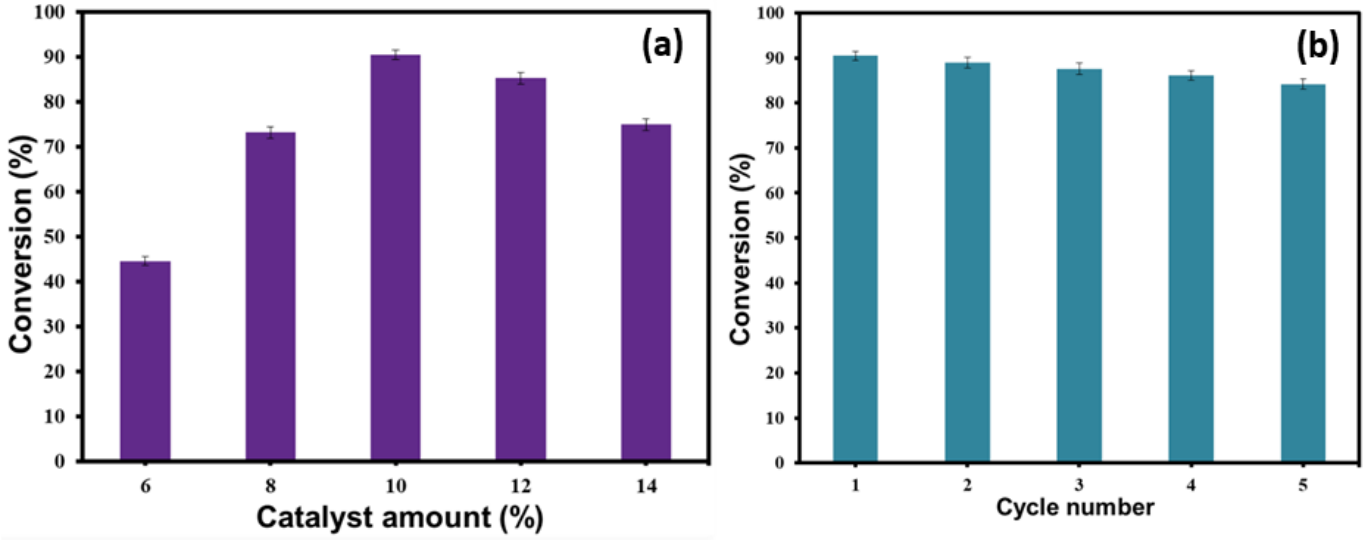

Figure 9. (**a**) Conversion of WCO at different catalyst doses (6 to 14 wt%), 15:1 methanol/oil molar ratio, 8 h reaction time and 180 °C temperature and (**b**) Reusability results of the synthesized (10 wt%)Ni–ZrO_2 catalyst toward biodiesel production from WCO, 15:1 methanol/oil molar ratio, 10 wt% catalyst concentration, 8 h reaction time and 180 °C temperature.

In some cases, a high amount of catalyst in the identical ratio of oil and methanol led to a lower mixing producing higher viscosity of the mixture of reactants and catalyst. The resultant increase in mass transfer resistance could reduce the biodiesel yield [63]. Therefore, the optimal catalyst dosage utilized for biodiesel production was selected to be 10 wt%.

3.7. Catalyst Recovery Evaluation

The recyclability tests were carried out by employing the (10 wt%)Ni–ZrO_2 catalyst for several reactions (up to five cycles) under the optimized conditions (Figure 9b). After the accomplishment of every reaction, the residual catalyst was isolated by centrifugation and washed away with hexane. Furthermore, to clean the catalysts from other impurities, the catalysts were also washed with methanol [64]. The results showed that the WCO conversion was reduced by almost 6% after 5 reactions. The reduced catalytic activity can presumably be credited to the inevitable catalyst weight loss during purification. However, the fabricated catalyst was active and recyclable even after five cycles of the transesterification process.

4. Conclusions

In this paper, we have synthesized (X%)Ni–ZrO_2 (X = 10, 25 and 50 wt%) catalysts using the green and scalable solvothermal procedure. The prepared materials were employed for the transesterification reaction of WCO with methanol to obtain biodiesel. The structures and compositions of the as-synthesized materials were characterized by different microscopic and spectroscopic techniques. The influence of several reaction factors, including catalyst loading, MeOH to oil molar ratio, reaction time, the catalyst to oil ratio, and reaction temperature, are thoroughly optimized. The optimal conditions for biodiesel production are a MeOH to oil molar ratio of 15:1, a catalyst to oil ratio of 10 wt%, a reaction temperature of 180 °C and a reaction time of 8 h. under these conditions. The transesterification resulted in a high FAME yield of 90.5%. The (10 wt%)Ni–ZrO_2 catalyst possesses the highest surface area compared to the un-doped catalyst (i.e., pure ZrO_2), and

the higher Ni-containing catalyst exhibited the maximum conversion of WCO to biodiesel. In addition, the (10 wt%)Ni–ZrO_2 catalyst was stable and could be successfully recycled five subsequent times with a marginal decline in its effectiveness. Additionally, the easy separation and recyclability of the catalyst after the reaction added another advantage to the prepared catalyst.

Author Contributions: Conceptualization, M.N.T. and S.F.A.; methodology, M.N.T. and S.F.A.; validation, J.V.S.K., A.A.-W. and M.R.H.S.; formal analysis, M.A., M.K. (Majad Khan), M.E.A. and A.K.; investigation, M.R.S., M.K. (Mufsir Kuniyil) and M.E.A.; resources, A.A.-W. and S.F.A.; data curation, M.R.S., M.K. (Mujeeb Khan) and M.K. (Mufsir Kuniyil); writing—original draft preparation, M.R.S., M.N.T. and S.F.A.; writing—review and editing, M.R.S., M.K. (Mujeeb Khan), M.N.T. and S.F.A.; visualization M.N.T. and S.F.A.; supervision, A.A.-W. and M.R.H.S.; project administration, S.F.A.; funding acquisition, S.F.A. All authors have read and agreed to the published version of the manuscript.

Funding: The authors extend their appreciation to the Deputyship for Research & Innovation, Ministry of Education in Saudi Arabia for funding this research work through the project no. (IFKSURG-2-1115).

Institutional Review Board Statement: Not Applicable.

Informed Consent Statement: Not Applicable.

Data Availability Statement: The data contained within the article.

Acknowledgments: The authors extend their appreciation to the Deputyship for Research & Innovation, Ministry of Education in Saudi Arabia for funding this research work through the project no. (IFKSURG-2-1115).

Conflicts of Interest: The authors declare no conflict of interest.

References

1. Ali, C.H.; Qureshi, A.S.; Mbadinga, S.M.; Liu, J.-F.; Yang, S.-Z.; Mu, B.-Z. Biodiesel production from waste cooking oil using onsite produced purified lipase from Pseudomonas aeruginosa FW_SH-1: Central composite design approach. *Renew. Energy* **2017**, *109*, 93–100. [CrossRef]
2. Ahmad, T.; Danish, M.; Kale, P.; Geremew, B.; Adeloju, S.B.; Nizami, M.; Ayoub, M. Optimization of process variables for biodiesel production by transesterification of flaxseed oil and produced biodiesel characterizations. *Renew. Energy* **2019**, *139*, 1272–1280. [CrossRef]
3. Macina, A.; de Medeiros, T.V.; Naccache, R. A carbon dot-catalyzed transesterification reaction for the production of biodiesel. *J. Mater. Chem. A* **2019**, *7*, 23794–23802. [CrossRef]
4. Atabani, A.E.; Silitonga, A.S.; Badruddin, I.A.; Mahlia, T.M.I.; Masjuki, H.H.; Mekhilef, S. A comprehensive review on biodiesel as an alternative energy resource and its characteristics. *Renew. Sustain. Energy Rev.* **2012**, *16*, 2070–2093. [CrossRef]
5. Uprety, B.K.; Chaiwong, W.; Ewelike, C.; Rakshit, S.K. Biodiesel production using heterogeneous catalysts including wood ash and the importance of enhancing byproduct glycerol purity. *Energy Convers. Manag.* **2016**, *115*, 191–199. [CrossRef]
6. Hamze, H.; Akia, M.; Yazdani, F. Optimization of biodiesel production from the waste cooking oil using response surface methodology. *Process Saf. Environ. Prot.* **2015**, *94*, 1–10. [CrossRef]
7. Lee, A.F.; Bennett, J.A.; Manayil, J.C.; Wilson, K. Heterogeneous catalysis for sustainable biodiesel production via esterification and transesterification. *Chem. Soc. Rev.* **2014**, *43*, 7887–7916. [CrossRef]
8. Ganjehkaviri, A.; Jaafar, M.; Nazri, M.; Hosseini, S.E.; Musthafa, A.B. Performance evaluation of palm oil-based biodiesel combustion in an oil burner. *Energies* **2016**, *9*, 97. [CrossRef]
9. Singh, S.; Singh, D. Biodiesel production through the use of different sources and characterization of oils and their esters as the substitute of diesel: A review. *Renew. Sustain. Energy Rev.* **2010**, *14*, 200–216. [CrossRef]
10. Mofijur, M.; Masjuki, H.H.; Kalam, M.; Atabani, A.E.; Fattah, I.R.; Mobarak, H. Comparative evaluation of performance and emission characteristics of Moringa oleifera and Palm oil based biodiesel in a diesel engine. *Ind. Crops Prod.* **2014**, *53*, 78–84. [CrossRef]
11. Mihaela, P.; Josef, R.; Monica, N.; Rudolf, Z. Perspectives of safflower oil as biodiesel source for South Eastern Europe (comparative study: Safflower, soybean and rapeseed). *Fuel* **2013**, *111*, 114–119. [CrossRef]
12. Onoji, S.E.; Iyuke, S.E.; Igbafe, A.I.; Nkazi, D.B. Rubber seed oil: A potential renewable source of biodiesel for sustainable development in sub-Saharan Africa. *Energy Convers. Manag.* **2016**, *110*, 125–134. [CrossRef]
13. Teo, S.H.; Rashid, U.; Taufiq-Yap, Y.H. Biodiesel production from crude Jatropha Curcas oil using calcium based mixed oxide catalysts. *Fuel* **2014**, *136*, 244–252. [CrossRef]

14. Dueso, C.; Muñoz, M.; Moreno, F.; Arroyo, J.; Gil-Lalaguna, N.; Bautista, A.; Gonzalo, A.; Sánchez, J.L. Performance and emissions of a diesel engine using sunflower biodiesel with a renewable antioxidant additive from bio-oil. *Fuel* **2018**, *234*, 276–285. [CrossRef]
15. Veljković, V.B.; Biberdžić, M.O.; Banković-Ilić, I.B.; Djalović, I.G.; Tasić, M.B.; Nježić, Z.B.; Stamenković, O.S. Biodiesel production from corn oil: A review. *Renew. Sustain. Energy Rev.* **2018**, *91*, 531–548. [CrossRef]
16. Mansir, N.; Teo, S.H.; Rabiu, I.; Taufiq-Yap, Y.H. Effective biodiesel synthesis from waste cooking oil and biomass residue solid green catalyst. *Chem. Eng. J.* **2018**, *347*, 137–144. [CrossRef]
17. Balat, M.; Balat, H. Progress in biodiesel processing. *Appl. Energy* **2010**, *87*, 1815–1835. [CrossRef]
18. Sánchez-Arreola, E.; Bach, H.; Hernández, L.R. Biodiesel production from Cascabela ovata seed oil. *Bioresour. Technol. Rep.* **2019**, *7*, 100220. [CrossRef]
19. Verziu, M.; Coman, S.M.; Richards, R.; Parvulescu, V.I. Transesterification of vegetable oils over CaO catalysts. *Catal. Today* **2011**, *167*, 64–70. [CrossRef]
20. Lacome, T.; Hillion, G.; Delfort, B.; Revel, R.; Leporq, S.; Acakpo, G. Process for Transesterification of Vegetable or Animal Oils Using Heterogeneous Catalysts Based on Titanium, Zirconium or Antimony and Aluminium. U.S. Patent 7592470B2, 26 May 2004.
21. Cho, H.J.; Kim, S.H.; Hong, S.W.; Yeo, Y.-K. A single step non-catalytic esterification of palm fatty acid distillate (PFAD) for biodiesel production. *Fuel* **2012**, *93*, 373–380. [CrossRef]
22. Zou, H.; Lei, M. Optimum process and kinetic study of Jatropha curcas oil pre-esterification in ultrasonical field. *J. Taiwan Inst. Chem. Eng.* **2012**, *43*, 730–735. [CrossRef]
23. Wang, Z.-M.; Lee, J.-S.; Park, J.-Y.; Wu, C.-Z.; Yuan, Z.-H. Optimization of biodiesel production from trap grease via acid catalysis. *Korean J. Chem. Eng.* **2008**, *25*, 670–674. [CrossRef]
24. Ni, J.; Meunier, F. Esterification of free fatty acids in sunflower oil over solid acid catalysts using batch and fixed bed-reactors. *Appl. Catal. A Gen.* **2007**, *333*, 122–130. [CrossRef]
25. Chung, Z.L.; Tan, Y.H.; San Chan, Y.; Kansedo, J.; Mubarak, N.; Ghasemi, M.; Abdullah, M.O. Life cycle assessment of waste cooking oil for biodiesel production using waste chicken eggshell derived CaO as catalyst via transesterification. *Biocatal. Agric. Biotechnol.* **2019**, *21*, 101317. [CrossRef]
26. Asri, N.P.; Machmudah, S.; Budikarjono, K.; Roesyadi, A.; Goto, M. Palm oil transesterification in sub-and supercritical methanol with heterogeneous base catalyst. *Chem. Eng. Process.* **2013**, *72*, 63–67. [CrossRef]
27. Wong, Y.; Tan, Y.; Taufiq-Yap, Y.; Ramli, I. Effect of calcination temperatures of CaO/Nb_2O_5 mixed oxides catalysts on biodiesel production. *Sains Malays.* **2014**, *43*, 783–790.
28. Gurunathan, B.; Ravi, A. Biodiesel production from waste cooking oil using copper doped zinc oxide nanocomposite as heterogeneous catalyst. *Bioresour. Technol.* **2015**, *188*, 124–127. [CrossRef]
29. Mohadesi, M.; Aghel, B.; Maleki, M.; Ansari, A. Production of biodiesel from waste cooking oil using a homogeneous catalyst: Study of semi-industrial pilot of microreactor. *Renew. Energy* **2019**, *136*, 677–682. [CrossRef]
30. Putra, M.D.; Irawan, C.; Ristianingsih, Y.; Nata, I.F. A cleaner process for biodiesel production from waste cooking oil using waste materials as a heterogeneous catalyst and its kinetic study. *J. Clean. Prod.* **2018**, *195*, 1249–1258. [CrossRef]
31. Sadaf, S.; Iqbal, J.; Ullah, I.; Bhatti, H.N.; Nouren, S.; Nisar, J.; Iqbal, M. Biodiesel production from waste cooking oil: An efficient technique to convert waste into biodiesel. *Sustain. Cities Soc.* **2018**, *41*, 220–226.
32. Asri, N.P.; Sari, D.A.P.; Poedjojono, B.; Suprapto, A. Utilization of waste cooking oil for biodiesel production using alumina supported Base catalyst. In Proceedings of the 3rd International Conference on Biological, Chemical and Environmental Sciences, (BCES-2015), Kuala Lumpur, Malaysia, 21–22 September 2015.
33. Zabeti, M.; Daud, W.M.A.W.; Aroua, M.K. Activity of solid catalysts for biodiesel production: A review. *Fuel Process. Technol.* **2009**, *90*, 770–777. [CrossRef]
34. Chung, K.-H.; Chang, D.-R.; Park, B.-G. Removal of free fatty acid in waste frying oil by esterification with methanol on zeolite catalysts. *Bioresour. Technol.* **2008**, *99*, 7438–7443. [CrossRef] [PubMed]
35. Silva, C.C.C.; Ribeiro, N.F.; Souza, M.M.; Aranda, D.A. Biodiesel production from soybean oil and methanol using hydrotalcites as catalyst. *Fuel Process. Technol.* **2010**, *91*, 205–210. [CrossRef]
36. Braos-Garcıa, P.; Maireles-Torres, P.; Rodrıguez-Castellón, E.; Jiménez-López, A. Gas-phase hydrogenation of acetonitrile on zirconium-doped mesoporous silica-supported nickel catalysts. *J. Mol. Catal. A Chem.* **2003**, *193*, 185–196. [CrossRef]
37. Znak, L.; Stołecki, K.; Zieliński, J. The effect of cerium, lanthanum and zirconium on nickel/alumina catalysts for the hydrogenation of carbon oxides. *Catal. Today* **2005**, *101*, 65–71. [CrossRef]
38. Rodrıguez-Castellón, E.; Dıaz, L.; Braos-Garcıa, P.; Mérida-Robles, J.; Maireles-Torres, P.; Jiménez-López, A.; Vaccari, A. Nickel-impregnated zirconium-doped mesoporous molecular sieves as catalysts for the hydrogenation and ring-opening of tetralin. *Appl. Catal. A Gen.* **2003**, *240*, 83–94. [CrossRef]
39. Jalowiecki-Duhamel, L.; Zarrou, H.; D'Huysser, A. Low temperature hydrogen production from methane on cerium nickel-and zirconium-based oxyhydrides. *Catal. Today* **2008**, *138*, 124–129. [CrossRef]
40. Assal, M.E.; Shaik, M.R.; Kuniyil, M.; Khan, M.; Al-Warthan, A.; Siddiqui, M.R.H.; Khan, S.M.; Tremel, W.; Tahir, M.N.; Adil, S.F. A highly reduced graphene oxide/ZrO_x–$MnCO_3$ or–Mn_2O_3 nanocomposite as an efficient catalyst for selective aerial oxidation of benzylic alcohols. *RSC Adv.* **2017**, *7*, 55336–55349. [CrossRef]

41. Gohel, V.D.; Rajput, A.; Gahlot, S.; Kulshrestha, V. Removal of Toxic Metal Ions From Potable Water by Graphene Oxide Composites. *Macromol. Symp.* **2017**, *376*, 1700050. [CrossRef]
42. Blair, A.C.; Weston, L.A.; Nissen, S.J.; Brunk, G.R.; Hufbauer, R.A. The importance of analytical techniques in allelopathy studies with the reported allelochemical catechin as an example. *Biol. Invasions* **2009**, *11*, 325–332. [CrossRef]
43. Chen, H.; Meng, Y.; Jia, S.; Hua, W.; Cheng, Y.; Lu, J.; Wang, H. Graphene oxide modified waste newspaper for removal of heavy metal ions and its application in industrial wastewater. *Mater. Chem. Phys.* **2020**, *244*, 122692. [CrossRef]
44. Smirnov, A.; Pinargote, S.; Washington, N.; Peretyagin, N.; Pristinskiy, Y.; Peretyagin, P.; Bartolomé, J.F. Zirconia Reduced Graphene Oxide Nano-Hybrid Structure Fabricated by the Hydrothermal Reaction Method. *Materials* **2020**, *13*, 687. [CrossRef] [PubMed]
45. Gurushantha, K.; Anantharaju, K.; Renuka, L.; Sharma, S.; Nagaswarupa, H.; Prashantha, S.; Vidya, Y.; Nagabhushana, H. New green synthesized reduced graphene oxide–ZrO_2 composite as high performance photocatalyst under sunlight. *RSC Adv.* **2017**, *7*, 12690–12703. [CrossRef]
46. Adil, S.F.; Assal, M.E.; Shaik, M.R.; Kuniyil, M.; AlOtaibi, N.M.; Khan, M.; Sharif, M.; Alam, M.M.; Al-Warthan, A.; Mohammed, J.A. A Facile Synthesis of ZrOx-$MnCO_3$/Graphene Oxide (GRO) Nanocomposites for the Oxidation of Alcohols using Molecular Oxygen under Base Free Conditions. *Catalysts* **2019**, *9*, 759. [CrossRef]
47. Elshazly, E.S.; Abdelal, O.A. Nickel stabilized zirconia for SOFCs: Synthesis and characterization. *Int. J. Metall. Eng.* **2012**, *1*, 130–134. [CrossRef]
48. Kanthimathi, M.; Dhathathreyan, A.; Nair, B. Nanosized nickel oxide using bovine serum albumin as template. *Mater. Lett.* **2004**, *58*, 2914–2917. [CrossRef]
49. Sun, H.; Ding, Y.; Duan, J.; Zhang, Q.; Wang, Z.; Lou, H.; Zheng, X. Transesterification of sunflower oil to biodiesel on ZrO_2 supported La_2O_3 catalyst. *Bioresour. Technol.* **2010**, *101*, 953–958. [CrossRef]
50. Dahdah, E.; Estephane, J.; Haydar, R.; Youssef, Y.; El Khoury, B.; Gennequin, C.; Aboukaïs, A.; Abi-Aad, E.; Aouad, S. Biodiesel production from refined sunflower oil over Ca–Mg–Al catalysts: Effect of the composition and the thermal treatment. *Renew. Energy* **2020**, *146*, 1242–1248. [CrossRef]
51. Knothe, G. Analytical methods used in the production and fuel quality assessment of biodiesel. *Trans. ASAE* **2001**, *44*, 193. [CrossRef]
52. Gelbard, G.; Bres, O.; Vargas, R.; Vielfaure, F.; Schuchardt, U. ^{1}H nuclear magnetic resonance determination of the yield of the transesterification of rapeseed oil with methanol. *J. Am. Oil Chem. Soc.* **1995**, *72*, 1239–1241. [CrossRef]
53. Srinivas, D.; Satyarthi, J.K. Biodiesel Production from Vegetable Oils and Animal Fat over Solid Acid Double-Metal Cyanide Catalysts. *Catal. Surv. Asia* **2011**, *15*, 145–160. [CrossRef]
54. Jacobson, K.; Gopinath, R.; Meher, L.C.; Dalai, A.K. Solid acid catalyzed biodiesel production from waste cooking oil. *Appl. Catal. B Environ.* **2008**, *85*, 86–91. [CrossRef]
55. Đặng, T.-H.; Chen, B.-H.; Lee, D.-J. Optimization of biodiesel production from transesterification of triolein using zeolite LTA catalysts synthesized from kaolin clay. *J. Taiwan Inst. Chem. Eng.* **2017**, *79*, 14–22. [CrossRef]
56. Amani, H.; Ahmad, Z.; Asif, M.; Hameed, B. Transesterification of waste cooking palm oil by MnZr with supported alumina as a potential heterogeneous catalyst. *J. Ind. Eng. Chem.* **2014**, *20*, 4437–4442. [CrossRef]
57. Feyzi, M.; Shahbazi, Z. Preparation, kinetic and thermodynamic studies of Al–Sr nanocatalysts for biodiesel production. *J. Taiwan Inst. Chem. Eng.* **2017**, *71*, 145–155. [CrossRef]
58. Ayoub, M.; Bhat, A.H.; Ullah, S.; Ahmad, M.; Uemura, Y. Optimization of biodiesel production over alkaline modified clay catalyst. *J. Jpn. Inst. Energy* **2017**, *96*, 456–462. [CrossRef]
59. Teo, S.H.; Islam, A.; Ng, C.H.; Mansir, N.; Ma, T.; Choong, S.T.; Taufiq-Yap, Y.H. Methoxy-functionalized mesostructured stable carbon catalysts for effective biodiesel production from non-edible feedstock. *Chem. Eng. J.* **2018**, *334*, 1851–1868. [CrossRef]
60. Amani, H.; Ahmad, Z.; Hameed, B. Highly active alumina-supported Cs–Zr mixed oxide catalysts for low-temperature transesterification of waste cooking oil. *Appl. Catal. A Gen.* **2014**, *487*, 16–25. [CrossRef]
61. Xie, W.; Peng, H.; Chen, L. Calcined Mg–Al hydrotalcites as solid base catalysts for methanolysis of soybean oil. *J. Mol. Catal. A Chem.* **2006**, *246*, 24–32. [CrossRef]
62. Marinković, D.M.; Stanković, M.V.; Veličković, A.V.; Avramović, J.M.; Miladinović, M.R.; Stamenković, O.O.; Veljković, V.B.; Jovanović, D.M. Calcium oxide as a promising heterogeneous catalyst for biodiesel production: Current state and perspectives. *Renew. Sustain. Energy Rev.* **2016**, *56*, 1387–1408. [CrossRef]
63. Saba, T.; Estephane, J.; El Khoury, B.; El Khoury, M.; Khazma, M.; El Zakhem, H.; Aouad, S. Biodiesel production from refined sunflower vegetable oil over KOH/ZSM5 catalysts. *Renew. Energy* **2016**, *90*, 301–306. [CrossRef]
64. Kaur, N.; Ali, A. Preparation and application of $Ce/ZrO_2-TiO_2/SO_4^{2-}$ as solid catalyst for the esterification of fatty acids. *Renew. Energy* **2015**, *81*, 421–431. [CrossRef]